DOI: 10.1002/chem.200802591

A Novel Tripodal Ligand Containing Three Different *N*-Heterocyclic Donor Functions and Its Application in Catechol Dioxygenase Mimicking

Marit Wagner, Christian Limberg,* and Thomas Tietz[a]

Dedicated to Professor Joachim Sauer on the occasion of his 60th birthday

Abstract: We describe a novel chiral ligand, **L**, in which three different *N*-donor functions are linked to a methoxymethine unit: a methylpyrazole derivative, a methylimidazole unit, and a pyridyl residue. Complexes with $FeCl_2$, $FeBr_2$, and $FeCl_3$ have been synthesized and fully characterized, including with respect to their molecular structures. While in combination with $FeCl_3$ **L** coordinates in a tripodal fashion, with FeX_2 (X = Cl, Br) it binds only through two functions and the pyridyl unit remains dangling. For potential modelling of intradiol and extradiol catechol dioxygenase reactivity, the complexes [$LFeCl_2$], **1**, and [$LFeCl_3$], **3**, have been treated with 3,5-di-*tert*-butylcatechol, triethylamine, and O_2. Both complexes yielded similar results in such investigations, since the LFe^{II}–catecholate complex reacts with O_2 through one-electron oxidation in the first step. Employing **3** in acetonitrile solution, intradiol cleavage occurred, although the undesired quinone was formed as the main product. If reagents were added ($NaBPh_4$, H^+) or reaction conditions were chosen (CH_2Cl_2 instead of CH_3CN as the solvent) that made the coordination sphere at the iron centre more accessible for a third substrate donor function, an alternative reaction route, presumably involving O_2 binding at the metal, became more important, which led to extradiol cleavage. In the extreme case (CH_2Cl_2 as the solvent and with the addition of $NaBPh_4$), mainly the extradiol cleavage products were formed; the intradiol products were only observed as side products then and quinone formation became negligible. Protonated base functions in the second coordination sphere increased the efficiency of extradiol cleavage only slightly. The obtained results are in line with current understanding of the function of intradiol/extradiol dioxygenases.

Keywords: coordination modes · iron · N ligands · O–O activation · reaction mechanisms

Introduction

Histidine moieties are often found as ligands within the prosthetic groups of metalloenzymes.[1–3] A common binding motif is the so-called 2-histidine-1-carboxylate facial triad,[4] and in proteins such as tyrosinase,[1] carboanhydrase,[2] or hemeerythrin[3] as many as three histidine-based imidazole residues are coordinated to a single metal centre. This has inspired the design and employment of multipodal ligands with *N*-heterocyclic donor functions for biomimetic chemistry. For instance, Tp (tris(pyrazolyl)borate)[5] makes use of three pyrazole donors, while three imidazole units are found in tris(imidazolyl)methane.[6] Pyridyl-based ligands are also frequently used in this context, the best-known representative being tetrapodal TPA (tris(pyridylmethyl)amine), in which three pyridyl donors are linked to an amine.[7] The reaction pockets of metalloenzymes are intrinsically chiral, and although certain protein functions do not utilize this feature directly during substrate conversion, it allows for stereoselective reactions, for instance at the active centres of cytochrome P450[8] or the lipoxygenases.[9] We have therefore contemplated the synthesis of a chiral tripodal ligand that contains the donor functions central to biomimetic or bioinspired chemistry, namely imidazolyl, pyrazolyl, and pyridyl residues. Here, we report such a ligand, which contains one of each of these units, as well as its iron(II) and iron(III) chlorido complexes. Furthermore, we have investigated the reactivity of these compounds in O_2 activation reactions, and in order to get an idea concerning the potential of our novel ligand we have chosen a modelling target, in relation to which various ligands have already been employed (albeit it does not take advantage of the chirality of our ligand), namely the extradiol catechol dioxygenase (belonging to the 2-histidine-1-carboxylate family).[9]

[a] Dipl.-Chem. M. Wagner, Prof. Dr. C. Limberg, Dipl.-Chem. T. Tietz
Institut für Anorganische Chemie, Humboldt-Universität zu Berlin
Brook-Taylor-Str. 2, 12489 Berlin (Germany)
Fax: (+49) 030-2093-6966
E-mail: christian.limberg@chemie.hu-berlin.de

Supporting information for this article is available on the WWW under http://dx.doi.org/10.1002/chem.200802591.

Results and Discussion

Ligand synthesis: The ligand synthesis started from the ketone **I** (see Scheme 1), which has previously been prepared by Canty et al.[10] and already contains a pyridyl as well as an imidazolyl moiety. In order to attach a pyrazolyl unit, a suitable precursor, 3(5)-*tert*-butylpyrazole,[11] was first treated with formaldehyde to protect the NH unit.[12] The protected pyrazole was then deprotonated with 2 equiv of *n*BuLi and subsequent reaction with **I** yielded the alcohol **II**. As it was envisaged that the alcohol unit might disturb coordination through the three *N*-donor functions, **II** was further reacted with NaH and MeI in order to methylate all acidic functions. In this way, the potential ligand **L** containing three different *N*-donor functions connected to a methoxymethine unit was obtained. The central carbon atom in **L** is thus chiral, and the compound was obtained in the form of a racemic mixture. Analytical HPLC investigations showed that the enantiomers could be separated by employing a chiral AD-H column (mobile phase: hexane/isopropanol/triethylamine, 90:10:0.2), which, however, was not necessary for the present application concerning catechol oxygenation; this does not focus on the chirality, and so the mixture of isomers has been employed in all of the described studies.

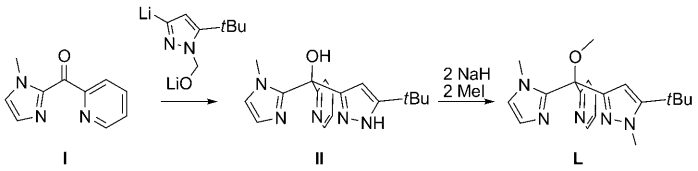

Scheme 1. Synthesis of the ligand **L**.

Complex synthesis: Treatment of **L** with $FeCl_2$ in THF led to the formation of the complex [$LFeCl_2$], **1** (Scheme 2), which has been characterized by IR spectroscopy, elemental analysis, and single-crystal X-ray diffraction analysis.

As found in the case of the other compounds containing **L** described below, crystals of **1** contained both enantiomers in the unit cell. Only the molecular structure of **1** with **L** in the (*S*)-configuration is shown in Figure 1.

Despite its three donor functions, the ligand coordinates in a bidentate fashion through the imidazolyl and pyrazolyl donors, while the pyridyl unit remains dangling. Iron(II) is known to form tetrahedral complexes quite often,[13] and apparently also in this case the iron centre does not require

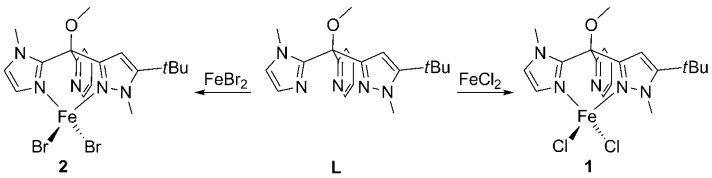

Scheme 2. Synthesis of the iron(II) complexes **1** and **2**.

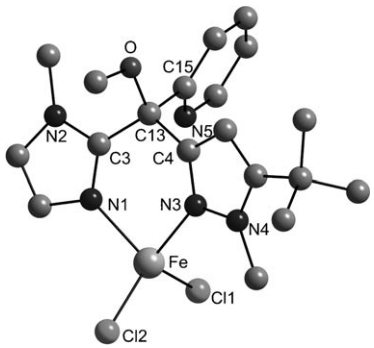

Figure 1. Molecular structure of [$LFeCl_2$] **1**. Hydrogen atoms are omitted for clarity. Selected bond lengths [Å] and angles [°]: Cl1-Fe 2.2607(10), Cl2–Fe 2.2409(11), Fe–N1 2.062(2), Fe–N3 2.081(2); N1-Fe-N3 86.06(9), N1-Fe-Cl2 107.59(7), N3-Fe-Cl2 116.02(8), N1-Fe-Cl1 117.74(7), N3-Fe-Cl1 110.58(8), Cl2-Fe-Cl1 115.57(5).

any further electronic saturation by coordination of a fifth donor function. However, it is not obvious why the pyridyl arm remains dangling as opposed to the pyrazole donor function. Hitchman et al. performed spectroscopic investigations of the metal binding at the tripodal ligand (pyrazolyl)$_2$-(pyridyl)CH and found that, in agreement with previous studies on the analogous monodentate ligands,[14a] the pyridine group in the tripodal ligand produces a slightly stronger interaction than either of the pyrazole groups.[14b] A favourable binding of the pyridine function of **L** would also be expected considering the pK_a values. Assuming that the degree of back-bonding is not very high (which is reasonable for Fe^{II}) and that all three donor functions have the same freedom to bind (with respect to steric constraints), the discussion may be focused on the free electron pairs interacting with the metal centre, which in turn might be comparable with H^+; in this case, the binding ability should correlate with the pK_a values, and that of pyridine (5.6) lies between those of 1-methylpyrazole (2.1) and 1-methylimidazole (7.2).[15] Hence, on this basis, the imidazole function should be the strongest donor and the pyridyl residue should bind ahead of the pyrazole entity. Against this background, the preferred binding of pyrazole can only be rationalized with reference to steric considerations. Assuming that, as the strongest donor, imidazole coordinates first, it would seem that a chelate with an additional σ-donor achieves a more favourable orbital interaction (aligned with the M–N vectors) if this donor is incorporated into the five-membered ring of pyrazole rather than the six-membered pyridyl ring. The angles at the iron centre of **1** vary between 86.06(9)° (N1-Fe-N3) and 117.75(7)° (N1-Fe-Cl1), indicating a significant distortion of the tetrahedral coordination sphere. The six-membered chelate ring is almost planar. Analogously to the synthesis of **1**, a corresponding bromide complex [$LFeBr_2$], **2**, could be prepared in 47% yield starting from $FeBr_2$ (Scheme 2). Single crystals could also be obtained for **2** by evaporating the solvent from a solution in THF, so that an X-ray diffraction study could be performed. All bond lengths and angles (see the Supporting Information, Figure S1) were found to be very similar to those in **1**.

Next, we turned our attention to iron(III). Addition of **L** to a solution of $FeCl_3$ in THF led to an orange-yellow suspension, from which [$LFeCl_3$], **3**, could be isolated in 68% yield (Scheme 3).

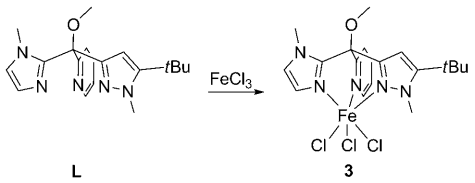

Scheme 3. Synthesis of the iron(III) complex **3**.

Complex **3** has been extensively characterized, including by single-crystal X-ray diffraction analysis. The molecular structure is shown in Figure 2. As anticipated, **L** now coordinates to the iron centre through its three donor functions. Accordingly, together with the three chlorido ligands a distorted octahedral coordination sphere results, with angles at the iron centre ranging from 77.79(13)° (N3-Fe-N1) to 100.81(5)° (Cl2-Fe-Cl1). The bond between the iron atom and the imidazole nitrogen atom (Fe–N3) is the shortest (2.146(4) Å) of the iron–nitrogen bonds, while the distance of the iron centre to the nitrogen atom of the pyridyl residue is the longest (Fe–N5 2.321(3) Å).

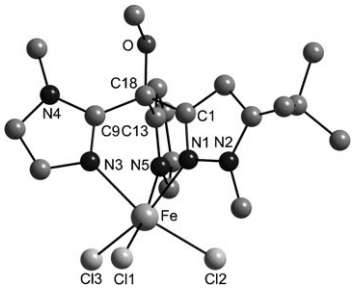

Figure 2. Molecular structure of [$LFeCl_3$] **3**. Hydrogen atoms are omitted for clarity. Selected bond lengths [Å] and angles [°]: Cl1–Fe 2.3009(12), Cl2–Fe 2.2795(13), Cl3–Fe 2.2962(12), Fe–N3 2.146(4), Fe–N1 2.172(3), Fe–N5 2.321(3); N3-Fe-N1 77.79(13), N1-Fe-Cl2 90.51(10), N3-Fe-Cl3 91.79(10), Cl2-Fe-Cl3 97.43(5), N3-Fe-Cl1 90.03(10), N1-Fe-Cl1 97.14(9), Cl2-Fe-Cl1 100.81(5), Cl3-Fe-Cl1 95.25(5), N3-Fe-N5 81.73(12), N1-Fe-N5 80.06(12), Cl2-Fe-N5 87.09(9), Cl3-Fe-N5 86.20(9), N3-Fe-Cl2 165.01(10), N1-Fe-Cl3 163.77(10), Cl1-Fe-N5 171.68(9).

Reactivity studies: As indicated in the introduction, the synthesized iron complexes have been tested with regard to their potential to model catechol dioxygenase reactivity, bearing in mind a comparison of **L** with other ligands employed in biomimetic chemistry. There are two classes of catechol dioxygenases: the extradiol catechol dioxygenases (EDO) and the intradiol catechol dioxygenases (IDO).[9] Both contain three amino acids bound at an iron centre; in the case of IDO one tyrosine and two histidine residues are coordinated to Fe^{III} (a further tyrosine residue has been shown to dissociate upon catechol binding),[9] while in the case of EDO one glutamate and two histidine units are bound to Fe^{II} (Scheme 4). Hence, after binding of the substrate catechol, their reaction mechanisms in the presence of O_2 are different, as are the products. IDO may be regarded as an Fe^{II}(semiquinone) complex (rather than an Fe^{III}-(catechol) substrate complex), with substantial radical character at its carbonyl C atoms, which are thus prone to attack by the biradical O_2, thereby yielding an anhydride. In contrast, the first step of the EDO system involves the binding and activation of O_2 at the Fe^{II} centre, which subsequently attacks the substrate to generate a lactone.[16]

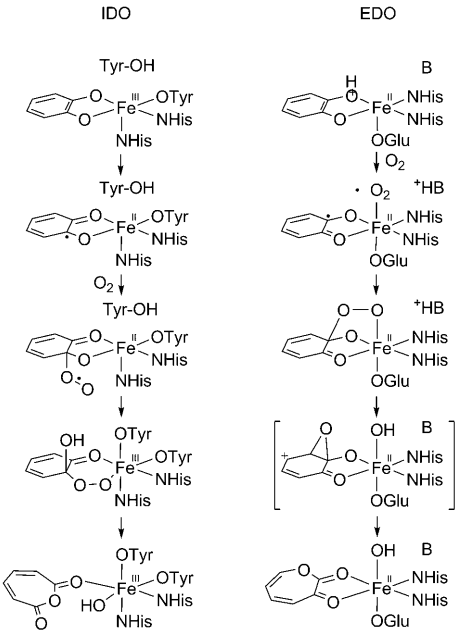

Scheme 4. Proposed reaction mechanisms for intradiol catechol dioxygenase (IDO) and extradiol catechol oxygenase (EDO).

Against this background, studies aimed at modelling IDO should strictly speaking should start from an Fe^{III}–catecholate complex, while the mimicking of EDO requires Fe^{II}–catecholate units. The few examples of crystallographically characterized Fe^{II}–catecholate complexes contain tetradentate ligands such as TPA, which, together with the bidentate substrate, occupy six coordination sites at the iron centre.[17] Hence, there is no free binding site for O_2 coordination and consequently catechol oxidation by O_2 cannot proceed in a biomimetic fashion. Fe^{II} is most probably first oxidized to Fe^{III} so that the subsequent oxidation process resembles that proposed for IDO; accordingly, the products of such reactions are often those expected for intradiol cleavage. The initial conversion of parent Fe^{II} models to Fe^{III} analogues can, however, also occur for Fe^{II} complexes containing tridentate ligands, which then also exhibit IDO beside EDO reactivity (due to insufficient site isolation being provided by the model ligand set).[18]

Various ligands have been employed for the preparation of [LFe^{III}(catecholate)] complexes as functional models for

IDO (derivatives of catechol such as 3,5-di-*tert*-butylcatechol, $DBCH_2$, are often employed), and some of these complexes have been well characterized.[19,20] In reactions with O_2, such complexes can lead to various products, the most undesirable (but often unavoidable) of which is the auto-oxidation product quinone **Q**.

The product expected for IDO reactivity would be **A** (3,5-di-*tert*-butyl-1-oxacyclohepta-3,5-diene-2,7-dione; Scheme 5) or its hydrolysis product 3,5-di-*tert*-butyl-5-(carboxymethyl)-2-furanone. Most IDO models with tridentate ligands tend to generate **A** along with the extradiol cleavage products **B** (4,6-di-*tert*-butyl-2-pyrone) and **C** (3,5-di-*tert*-butyl-2-pyrone), which are obtained as the main products (they are generated through the EDO pathway followed by CO elimination).[19] To explain this, it has been suggested that the alkyl peroxide intermediate formed from such Fe^{III}–IDO models can decompose via two pathways, and that subtle influences determine the ultimate product selectivity (see below). Only [LFe^{III}(dbc)] complexes, in which L is a tetradentate ligand, selectively lead to **A**.[20]

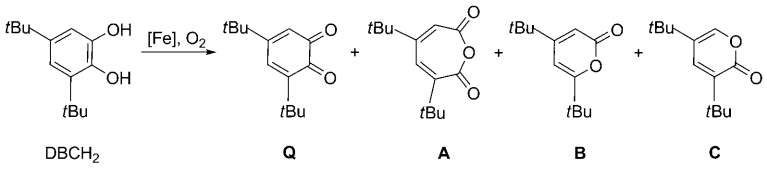

Scheme 5. Products of the oxidative cleavage of 3,5-di-*tert*-butylcatechol.

Complex **1** contains an iron(II) centre bound by **L**, and after further coordination by $DBCH^-$ the resulting complex might thus be regarded as an EDO model. Hence, to simulate the situation shown on the right-hand site of Scheme 4 we first treated **1** with $DBCH_2$ in the presence of one equivalent of NEt_3, which led to a vinaceous wine-red solution. Attempts to follow the reaction by means of NMR spectroscopy did not, however, lead to any further information due to the large half widths of the paramagnetically shifted signals leading to substantial overlap. Addition of O_2 to such a solution led to an immediate colour change to purple, which was monitored by UV/Vis spectrophotometry. After 20 min, new bands had appeared at around 545 nm ($\varepsilon = 1480\,M^{-1}cm^{-1}$) and 837 nm ($\varepsilon = 1560\,M^{-1}cm^{-1}$), which were similar to those observed for the independently synthesized [LFe^{III}(dbc)Cl] complex (554 nm, $\varepsilon = 1377\,M^{-1}cm^{-1}$; 813 nm, $\varepsilon = 1347\,M^{-1}cm^{-1}$; see the Supporting Information, Figure S2). The latter two bands could be assigned to catecholato–iron(III) LMCT transitions, which are characteristic of such moieties.[21] Such rapid Fe^{II}-to-Fe^{III}–catecholato oxidations upon exposure to O_2 have been observed before (see above) and as a result of this transformation the reactivity found for LFe^{II}/DBC/O_2 systems will clearly be very similar to that observed for the corresponding LFe^{III}/DBC/O_2 systems.[18] Preliminary experiments (see the Supporting Information; Table S1) showed that this was also true in the case of the present system, and so all further experiments were carried out by starting directly from **3**.

Treating **3** with $DBCH_2$ and two equivalents of triethylamine in acetonitrile led to a colour change to purple, indicating the formation of a complex [LFe(dbc)Cl] (Scheme 6).

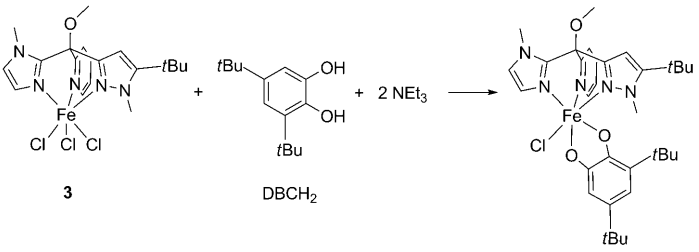

Scheme 6. Reaction of **3** with 3,5-di-*tert*-butylcatechol and triethylamine.

As yet, we have not been able to isolate and fully characterize this complex, but the colour and UV/Vis spectrum in acetonitrile (the bands and extinction coefficients quoted above are comparable to those of other DBC complexes[9]) as well as a peak at $m/z = 615.2860$ in the high-resolution ESI mass spectrum, which can be assigned to the ion [LFe(dbc)]$^+$ (m/z 615.2866), give good indications of its formation. Due to the three different N donor functions of **L**, three isomers can be expected upon binding of a chelating ligand to the $[LFeCl]^{2+}$ unit, and due to the asymmetric substitution pattern within DBC a further three are possible. Preliminary calculations (BP86/LANL2DZ) showed that the energies of the individual isomers vary within a range of 12.2 kJ mol^{-1} (see the Supporting Information, Table S2). Attempts to crystallize the product from such solutions led in one case to a small amount of crystals of **1** (slow evaporation of the solvent from a solution in diethyl ether of the product obtained from a reaction performed in dichloromethane), and in another case to crystals of $[Cl_2Fe(\mu\text{-dbc})_2FeCl_2][FeL_2]$, **4** (slow evaporation of the solvent after performing the reaction in acetonitrile; Figure 3). Comparison of the structural data of the $[FeL_2]$ moiety of **4** ($Fe-N_{Pz}$ 1.990(5) Å, $Fe-N_{Im}$ 2.007(5) Å, $Fe-N_{Py}$ 1.985(5) Å) with those of the complex cation $[L_2Fe]^{2+}$ of the independently synthesized iron(II) compound $[FeL_2(OTf)_2]$ (**5**) ($Fe-N_{Pz}$ 2.1093(19) Å, $Fe-N_{Im}$ 2.0797(19) Å, $Fe-N_{Py}$ 2.194(2) Å; see the Supporting Information; Figure S4), as well as with those of the LFe^{3+} unit in **3**, points to an oxidation state of +II within the cation of **4**, so that the $[Cl_2Fe(\mu\text{-dbc})_2FeCl_2]$ moiety should bear a double negative charge. This is consistent with the observation that the compound $(lutidinium)_2[Cl_2Fe(\mu\text{-dbc})_2FeCl_2]$, with a similar anion, has been obtained from the reaction of $FeCl_3$ with 3,5-di-*tert*-butylcatechol and two equivalents of 2,6-lutidine in THF.[22]

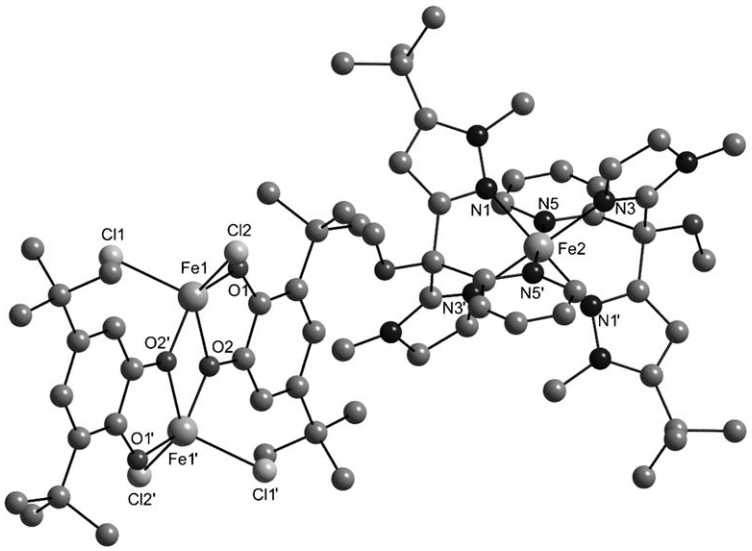

Figure 3. Molecular structure of $[Cl_2Fe(\mu\text{-dbc})_2FeCl_2][FeL_2]$, **4**. Hydrogen atoms are omitted for clarity. Selected bond lengths [Å] and angles [°]: Cl1–Fe1 2.2530(11), Cl2–Fe1 2.2691(12), Fe1–O1 1.909(3), Fe1–O2 2.030(3), Fe1–O2′ 2.011(2), Fe2–N1 2.000(3), Fe2–N3 2.008(3), Fe2–N5 1.974(3); O1-Fe1-O2 79.63(10), O1-Fe1-O2′ 149.19(11), O2-Fe1-O2′ 70.95(11), O1-Fe1-Cl1 103.58(9), O2-Fe1-Cl1 116.69(9), O2′-Fe1-Cl1 97.73(8), O1-Fe1-Cl2 95.89(9), O2-Fe1-Cl2 133.48(9), O2′-Fe1-Cl2 97.72(8), Cl1-Fe1-Cl2 109.41(5), N5-Fe2-N1 93.97(13), N5-Fe2-N1′ 86.03(13), N5-Fe2-N3 88.43(14), N5-Fe2-N3′ 91.57(14), N1-Fe2-N3 92.62(14), N1-Fe2-N3′ 87.38(13).

In the anion of **4** the two iron centres are each coordinated by two chlorido ligands, and they are bridged by two bidentate catecholato units, whereas in (lutidinium)$_2$[$Cl_2Fe(\mu\text{-dbc})_2FeCl_2$] the catecholate moieties bind only through one oxygen donor.

Although **1** and **4** were only isolated in small quantities as side-products, their formation shows that [LFe(dbc)Cl] is quite labile and slowly decomposes through redox reactions to give Fe^{II} compounds. This is not surprising as IDO reactivity is based on a catecholato-to-iron(III) electron transfer (see above). The degradation of 1:1 Fe^{III}–catecholate complexes to produce Fe^{II} has been reported previously, and as an acceleration by light was mentioned in this context,[23] the influence of light was also considered in the subsequent investigation of O_2 reactivity here. However, light did not seem to play a major role in our case (see below). For the reactivity studies with O_2 described below, it was assumed that the extent of decomposition during the reaction time was small, so that the concentrations of **1**, **4**, or other products of degradation could be regarded as negligible. This is important, since reactions of anions such as $[Cl_2Fe(\mu\text{-dbc})_2FeCl_2]^{2-}$ would surely lead mainly to **Q**; indeed, a test experiment showed that $FeCl_3$ reacted with DBC^{2-} and O_2 in acetonitrile within six hours to give almost exclusively **Q** (99%, accompanied by 1% **B**), which is in agreement with previous investigations.[24] ESI-MS studies confirmed the validity of the above assumption: upon addition of $DBCH_2$ and NEt_3 to a solution of **3** in acetonitrile, a peak at *m*/*z* 615.2860 immediately appeared and storage of the solution for 6 h did not lead to any further peaks.

Studies concerning the reactivity of [LFe(dbc)Cl] in the presence of O_2 were started as follows: **3**, $DBCH_2$, and NEt_3 in a ratio of 1:1:2 were dissolved in acetonitrile, excess O_2 was introduced, and the reaction was monitored by UV/Vis spectrophotometry (Figure 4). Both bands in the visible region (554 and 813 nm) decreased during the reaction and a new band developed at 379 nm, while an isosbestic point could be observed at 441 nm. As the concentration of dioxygen in the acetonitrile (8.1 mM)[20f] was much higher than that of the reacting complex (0.3 mM), the reaction conformed to pseudo-first-order kinetics with a rate constant of $k(O_2) = 0.0123\,M^{-1}s^{-1}$ (Figure 4). Within a reaction time of six hours, the original LMCT bands of the iron(III)–catecholato complex had disappeared almost completely. The rate constants found for other relevant systems,[20c,e,f,21] vary over three orders of magnitude and that found here falls at the lower end of the range. While one might expect to find a correlation between the CT band position and the reactivity, this is not evident: the rate constant measured here is significantly different from those found for complexes with similar CT band positions, and these in turn show great variations in reactivity among themselves.

For an analysis of the reaction products, all volatiles were removed from the reaction mixture after 6 h and the residue

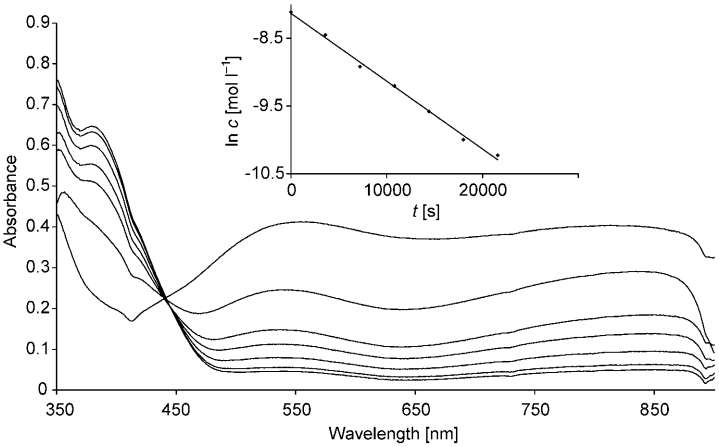

Figure 4. Evolution of the absorption spectrum upon exposure of **3** + $DBCH_2$ + 2NEt_3 to O_2 in MeCN. Spectra were recorded at hourly intervals. The top line shows the absorption spectrum of **3** + $DBCH_2$ + 2NEt_3. Inset: plot of ln*c* vs time.

Table 1. Oxidative catechol cleavage reactions with O_2.[a]

Entry	Solvent	$LFeCl_3$ (**3**)	Additive	**Q** [%]	**A** [%]	**B** [%]	**C** [%]	**B**+**C** [%]
1	MeCN	DBC^{2-}	–	63	34	3	–	3
2	MeCN	DBC^{2-}	–[b]	65	32	3	–	3
3	MeCN	DBC^{2-}	$NaBPh_4$	61	31	8	trace	8
4	CH_2Cl_2	DBC^{2-}	$NaBPh_4$	12	22	42	24	66
5	MeCN	$DBCH^-$	$NaBPh_4$	58	20	13	9	22
6	CH_2Cl_2	$DBCH^-$	$NaBPh_4$	6	23	43	28	71

[a] After 6 h reaction time, conversions for all reactions are between 77 and 85%. [b] The reaction was performed in the absence of light.

was extracted with $CHCl_3$. After filtration of the extract through silica gel, product yields were determined with the aid of ^1H NMR and GC-MS/FID (entry 1 in Table 1). It turned out that, under these conditions, mainly **Q** was formed, together with half as much **A**, the formation of which as a main product was not unexpected regarding **3** as an IDO model. Indeed, the yield of extradiol products was very low. Referring to the apparent instability of **3** in attempts to crystallize it, entry 2 describes an experiment in which the influence of light was tested (see above).[23] However, entries 1 and 2 are nearly identical, suggesting that light does not have any effect. Entry 3 in Table 1 addresses the influence of the coordination number at the iron centre, since the availability of a vacant site has been argued to be an essential factor for the occurrence of extradiol-type catechol cleavage:[16] O_2 then has the additional possibility of coordinating to the iron(II) centre generated in the course of electron transfer from the DBC ligand. Subsequently, an intermediate is formed, in which the organoperoxide unit is coordinated through three donor functions to an iron(III) centre (Scheme 7), in a fashion similar to that proposed for the EDO intermediate (cf. Scheme 4), in which, however, the iron atom is in the +II oxidation state.[16]

Accordingly, $NaBPh_4$ was added, with the intention of abstracting the residual chlorido ligand. In order to ensure that the appropriate reaction times were chosen, the reaction course was followed with time (aliquots were removed and analyzed). The results are shown in Figure 5.

The results obtained for **Q** and $DBCH_2$ are somewhat unreliable during the first hours of the conversion, as unreacted $DBCH_2$ is partly converted into **Q** during work-up. It is therefore more informative to concentrate on the other products. Evidently, the concentrations of **A** and **B** increase with increasing reaction time, but the yields obtained after three days are not much higher than those obtained after six hours. For further investigations, it thus seemed reasonable to continue comparing results obtained after 6 h, like those presented in Table 1, where entry 3 corresponds to the fourth measurement in Figure 5. It shows that the addition of $NaBPh_4$ does indeed somewhat decrease the yields of **A** and **Q** in favour of **B**; however, the effect is not very large, probably because acetonitrile solvent molecules occupy the free coordination sites. Hence, the same reaction was repeated in dichloromethane (entry 4), which led to dramatic changes: the yield of **Q** was significantly decreased, while the dioxygenase reactivity was changed from mainly intradiol to mainly extradiol. This is plausible since dichloromethane cannot occupy the free coordination site effectively, and apparently, as previously observed in cases of facially coordinating tridentate ligands,[19] this leads to a change in mechanism with respect to O_2 reactivity, as outlined above. Finally, the influence of the presence of protons was investigated for two reasons: first, it has been noted in investigations of models that the presence of protons may lead to the protonation of donor functions and thus to more spacious coordination spheres.[25] Secondly, it has been found in theoretical and experimental investigations concerning the native and mutated enzymes that the presence of a protonated histidine residue in the second coordination sphere is decisive for extradiol *vs* intradiol cleavage because it is thought to stabilize the iron–superoxo species,[26] to accelerate the attack of the bound superoxide on the substrate,[27] or to pro-

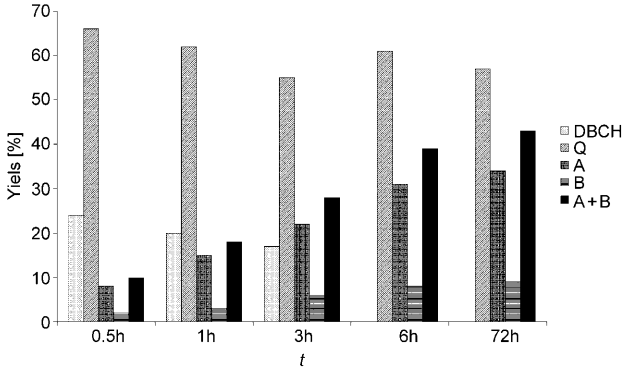

Figure 5. Temporal dependence of the product ratios of the reaction between **3**/DBC^{2-}/$NaBPh_4$ and O_2 in MeCN.

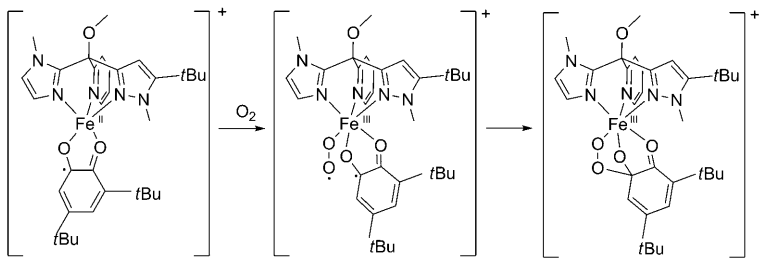

Scheme 7. Proposed mechanism for the reaction of **3** in the presence of $DBCH_2$, 2 NEt_3, $NaBPh_4$, and O_2.

mote alkenyl migration in the peroxo intermediate yielding the lactone species.[28] We have addressed this issue by studying the effect of reducing the amount of NEt_3 added to only one equivalent. Comparison of entries 1 and 5 shows that this somewhat decreased the yield of **A**, while more **B** and even some **C** were formed. A small increase in extradiol reactivity due to the presence of protons was also observed for solutions in dichloromethane (cf. entries 4 and 6). Hence, the effect of the presence of protons is greater than that of generating a free coordination site in acetonitrile, but smaller than that of a vacant site in dichloromethane.

Assuming that, for the reasons given above, there is a correlation between the space available at the metal centre and the extent of extradiol reactivity, these results can be rationalized as follows. In acetonitrile, a vacant site is immediately occupied by this solvent, so that hardly any difference is noted in comparison to chlorido coordination. The space generated by the free site is only available in dichloromethane, and this leads to significantly increased EDO reactivity. Addition of a proton (or more precisely omission of a base equivalent so that one of the $DBCH_2$ protons remains within the system) can be expected to have the two effects outlined above: (i) protonation of one ligand donor function, thereby generating a free coordination site, and (ii) an influence on the superoxide or peroxide intermediates that promote extradiol cleavage. A comparison of entries 4 and 6 allows evaluation of point (ii): the conditions of entry 4 are expected to produce $[LFe(dbc)]^+$ with a free coordination site, while those of entry 6 are likely to also produce a pentacoordinated iron centre, with the difference that **L** is only coordinated through two donor functions leaving one protonated base dangling; a chlorido ligand is left to coordinate instead. Hence, the situations in entries 4 and 6 differ in the availability of a protonated base function in the second coordination sphere, and this leads to an increase of the yields of extradiol products by 5%. Accordingly, the presence of BH^+ (B = base) has only a small effect. Applying the same arguments, entry 5 may be compared with entry 3, but a much larger influence (14%) is observed in this case, so that a further aspect must also play a role. While in the case of entry 3 acetonitrile can be expected to occupy the free coordination site generated, this might not be possible with the same efficiency in the case of entry 5 as the BH^+ remains in close proximity to the metal centre and blocks the linear coordination of acetonitrile to some extent (similar to the way in which a dangling His residue in hemoglobin disturbs the coordination of CO *vs* O_2).[29] Accordingly, a third coordination site is more readily available (albeit not completely as in the case of entry 4 since there is still competition with acetonitrile), and this increases the yield of extradiol products. If this hypothesis is correct, the space available at the iron centre systematically increases in the series of entries 1 $\rightarrow$ 3 $\rightarrow$ 5 $\rightarrow$ 4, and indeed the degree of extradiol reactivity increases in the same order. Entry 6 can be considered as the extreme case, since under these conditions the iron centre can be expected to have a free coordination site in addition to the beneficial influence of BH^+: consequently, hardly any formation of **Q** is observed and the extradiol reactivity reaches the highest value of 71%.

Intradiol cleavage seems to require only two coordination sites (for the coordination of DBC^{2-}) and was thus observed in all of the experiments.[30] The extent was highest (34%) when extradiol reactivity was basically excluded and somewhat smaller (20–23%) with competing extradiol cleavage. If extradiol reactivity is excluded through the lack of a free coordination site, only the formation of **Q** occurs simultaneously. With increasing available space, however, extradiol cleavage becomes more efficient than auto-oxidation, so that **Q** formation decreases in favour of extradiol cleavage.

Altogether, the results can be understood on the basis of previous hypotheses made by considering the reactivities of model compounds and native enzymes. Although there is a different order of initial events in the intradiol *vs* extradiol reaction mechanisms, they converge on a common proximal organoperoxide intermediate.[16] The two enzymes differ in the oxidation state of the iron centre within this intermediate, but considering the facts that the IDO pyrocatechase can perform extradiol cleavage when 3-methylcatechol is employed as the substrate[31] and that following mutation of certain EDOs (replacement of a His residue in the active site by Phe) intradiol cleavage is observed,[32] the choice of intradiol *vs* extradiol reaction pathways is clearly determined not so much by the iron oxidation states, but rather by stereoelectronic factors influencing the acyl *vs* alkenyl migration rearrangements of the organoperoxide intermediates.[16] The extradiol dioxygenase active site containing the His_2Glu motif is able to bind substrates and reaction intermediates through three coordination sites, and hence the organoperoxide intermediate may also be bound in a tridentate coordination mode (compare Scheme 4), that is, in a conformation in which the peroxide unit is positioned pseudoaxially.[16] This alignment allows for facial alkenyl migration and extradiol cleavage. The same can be deduced for iron(II) models containing facial tridentate ligands, as their coordination environment resembles the situation in the respective dioxygenase active site, and the conclusion even holds for iron(III) complexes: a comparable intermediate can be formed according to Scheme 7, and the influence of the oxidation state seems not to be decisive (see above). It is therefore plausible that a complex $[LFe(dbc)]^+$, as generated under the conditions outlined in entry 4, can show mainly extradiol reactivity, and thus compares well, for instance, with $[Tp^{iPr_2}Fe(dbc)]$ dissolved in toluene[18b] (considering that Tp is also a facially coordinating tripodal ligand) or with $[(BnBPA)Fe(dbc)]^+$ (BnBPA = *N*-benzyl *N*,*N*-bis(2-pyridylmethyl)amine) dissolved in dichloromethane.[19b] However, iron complexes with tetradentate ligands cannot react analogously, since only two coordination sites are available. This situation resembles that at the intradiol dioxygenase active site, where the His_2Tyr_2 motif provides four protein ligands for iron(III), provided that the tyrosyl unit coordinates after O_2 binding, as shown in Scheme 4.[16] The iron centre is then only capable of binding substrates and reaction intermediates through two coordination sites, that is

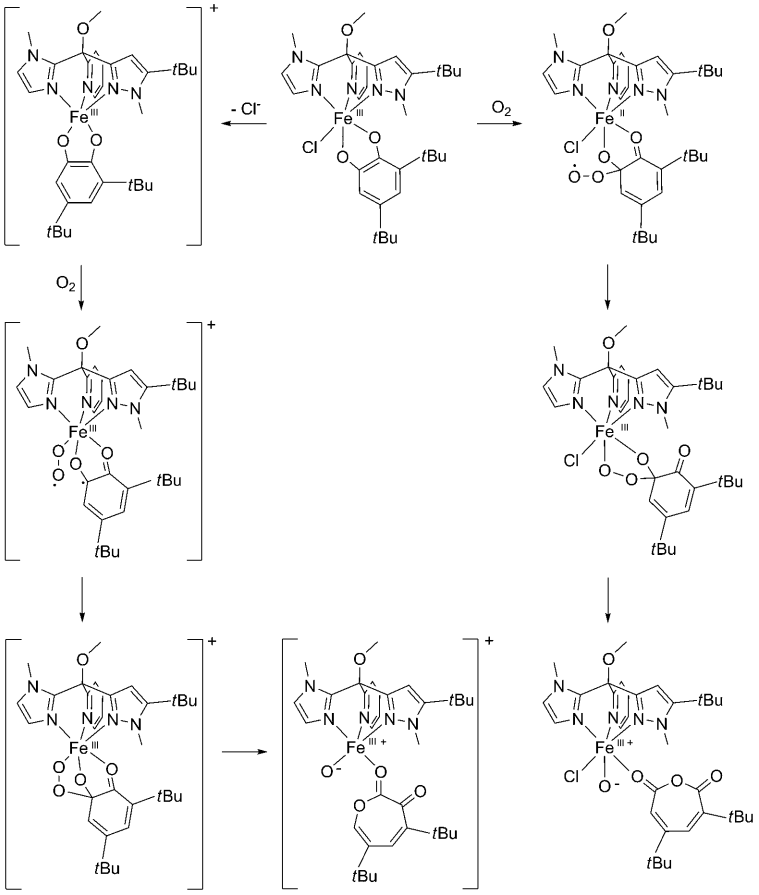

Scheme 8. Proposed reaction mechanisms of catechol cleavage for five- and six-coordinate complexes.

to say, the strict pseudo-axial peroxide conformation is more difficult to achieve and so acyl migration is favoured as opposed to alkenyl migration (Scheme 8).[16] Therefore, iron complexes with tetradentate ligands also represent selective catalysts for intradiol cleavage, and consistently the same is true for [LFe(dbc)Cl] (entry 1), in which, besides the tridentate ligand **L**, a chlorido ligand coordinates strongly to the iron centre.

Conclusion

A novel ligand, **L**, has been synthesized that shows interesting properties for application in bioinspired or biomimetic chemistry, as exemplified here for the case of catechol dioxygenase mimicking. The results obtained for the system $LFe^{3+}/DBCH_2/O_2$ under various conditions can be explained on the basis of the current concepts of understanding concerning the behaviour of native IDOs and EDOs, as well as the reactions of corresponding model complexes, and they show the general potential of **L** to model a histidine-rich facial triad in enzymes. Future research will be aimed at the synthesis of enantiomerically pure complexes of ligand **L** and their investigation with respect to enantioselective oxidations of prochiral substrates. To this end, we intend to synthesize derivatives of **L** in which the differences between the steric requirements of the individual donor functions are more pronounced so that stereochemical constraints are imposed more rigorously (for instance, by introducing a *tert*-butyl residue at the pyridyl ring).

Experimental Section

General: Apart from the ligand synthesis, all manipulations were carried out in a glove box, or else by means of Schlenk-type techniques involving the use of a dry argon atmosphere. The ^1H and ^{13}C NMR spectra were recorded on a Bruker AV 400 NMR spectrometer (^1H 400.13 MHz; ^{13}C 100.63 MHz) with $CDCl_3$ as solvent at 20 °C. The ^1H and ^{13}C NMR spectra were calibrated against the residual proton and natural abundance ^{13}C resonances of the deuterated solvent $CDCl_3$ (δ_H 7.26 ppm, δ_C 77.00 ppm). Microanalyses were performed on a Leco CHNS-932 elemental analyser or on a HEKAtech EURO EA. ESI mass spectra were recorded on an Agilent Technologies 6210 time-of-flight LC/MS. Infrared (IR) spectra were recorded with a Digilab Excalibur FTS 4000 FTIR spectrometer from samples prepared in KBr pellets. Solvents were dried using a Braun solvent purification system. (1-Methylimidazol-2-yl)(pyridin-2-yl)methanone (**I**),[9] 3(5)-*tert*-butyl-pyrazole,[10] 1-hydroxymethyl-3(5)-*tert*-butylpyrazole,[11] 3,5-di-*tert*-butyl-1-oxacyclohepta-3,5-diene-2,7-dione (**A**),[33] and 4,6-di-*tert*-butyl-2-pyrone (**B**)[34] were synthesized as described previously.

CCDC-711192, 711193, 711194, 711195, 711196, and 718663 contain the supplementary crystallographic data for this paper. These data can be obtained free of charge from The Cambridge Crystallographic Data Centre via www.ccdc.cam.ac.uk/data_request/cif.

2-[1-Hydroxy(1-methyl-1*H*-imidazol-2-yl)(1-methyl-5-*tert*-butylpyrazol-3-yl)methyl]pyridine (II): A 2.5 M solution of *n*BuLi in hexane (17.0 mL, 0.042 mol, 2 equiv) was slowly added to a solution of 1-hydroxymethyl-3(5)-*tert*-butylpyrazole (3.24 g, 0.021 mol) in THF at −78 °C. Following the addition, the reaction mixture was stirred for 1 h at −78 °C, and then for a further 1 h after warming to RT. After cooling to −60 °C, a solution of (1-methylimidazol-2-yl)(pyridin-2-yl)methanone (**I**) (4.00 g, 0.021 mol, 1 equiv) in THF was added. The colour of the solution quickly turned brown during this addition. After slowly warming to RT while stirring overnight, the mixture was neutralized with dilute aqueous hydrochloric acid and the phases were allowed to separate. The aqueous phase was extracted with dichloromethane (3×30 mL), and the combined organic phases were concentrated to dryness. The crude product thus obtained was dissolved in dichloromethane (10 mL) and the solution was overlayered with pentane (30 mL). Within 1 d, **II** had precipitated in the form of a white solid (3.30 g, 0.011 mol, 52 %). ^1H NMR ($CDCl_3$, 25 °C): $\delta = 1.27$ (s, 9H; $C(CH_3)_3$), 3.25 (s, 3H; Im N-CH_3), 6.02 (s, 1H; Pz CH-4), 6.82 (d, 1H, $J = 1.20$ Hz; Im CH-4/5), 6.90 (d, 1H, $J = 1.20$ Hz; Im CH-4/5), 7.26 (m, 1H; Py CH), 7.68 (m, 1H; Py CH), 7.71 (m, 1H; Py CH), 8.54 ppm (m, 1H; Py CH); ^{13}C NMR ($CDCl_3$, 25 °C): $\delta = 30.32$ ($C(CH_3)_3$), 31.42 (*C*-

(CH_3)$_3$), 34.49 (Im N-CH_3), 100.13 (Pz CH-4), 123.01 (Im CH-4/5), 123.16 (Im CH-4/5), 126.32 (Py CH), 137.02 (Py CH), 146.61 (Py CH), 159.23 ppm (Py CH); MS: *m*/*z*: 311 [M^+], 296, 278, 254, 233, 205, 188, 177, 151, 122, 106, 83; elemental analysis calcd (%) for $C_{17}H_{21}N_5O$: C 65.57, H 6.80, N 22.49; found: C 65.18, H 6.83, N 22.48.

2-[1-Methoxy(1-methylimidazol-2-yl)(1-methyl-5-*tert*-butylpyrazol-3-yl)-methyl]pyridine (L): NaH (850 mg, 35.4 mmol, 5.2 equiv) was added portionwise to a solution of the alcohol **II** (2.11 g, 6.77 mmol) in THF. The reaction mixture was stirred under argon for 7 d at RT and then heated to reflux for 5 h. After cooling to RT, iodomethane (1.5 mL, 24.1 mmol, 3.6 equiv) was added, and after stirring for a further 5 h all volatiles were removed under vacuum. Excess NaH was decomposed by treatment with water, and the resulting mixture was extracted with dichloromethane (3× 20 mL). Removal of the solvent from the combined extracts left the crude product as a yellow-brown solid, which could be purified by washing with THF to afford **L** in the form of a white powder (1.30 g, 3.83 mmol, 57%). ^{1}H NMR ($CDCl_3$, 25°C): δ=1.32 (s, 9H; C(CH_3)$_3$), 3.28 (s, 3H; Im N-CH_3), 3.31 (s, 3H; O-CH_3), 3.90 (s, 3H; Pz N-CH_3), 6.28 (s, 1H; Pz CH-4), 6.85 (d, 1H, *J*=1.19 Hz; Im CH-4/5), 7.05 (d, 1H, *J*=1.16 Hz; Im CH-4/5), 7.12 (m, 1H; Py CH), 7.66 (m, 1H; Py CH), 7.76 (m, 1H; Py CH), 8.53 ppm (m, 1H; Py CH); ^{13}C NMR ($CDCl_3$, 25°C): δ=29.55 (C(CH_3)$_3$), 31.06 (*C*(CH_3)$_3$), 34.02 (Im N-CH_3), 39.45 (Pz N-CH_3), 52.96 (O-CH_3), 81.57 (C_q-OCH_3), 104.62 (Pz CH-4), 121.85 (Py CH), 122.90 (Py CH), 122.81 (Im CH 4/5), 126.48 (Im CH 4/5), 136.12 (Py CH), 146.76 (Im C-2), 148.34 (Py CH), 149.50 (Pz C-3), 150.96 (Pz C-5), 161.69 ppm (Py C-2); IR (KBr): $\tilde{\nu}$=3050 (m), 2996 (m), 2974 (s), 2961 (s), 2950 (s), 2932 (m), 2927 (m), 2923 (m), 2909 (m), 2890 (m), 2887 (m), 2871 (m), 2821 (m), 1586 (m), 1527 (m), 1488 (m), 1468 (s), 1437 (m), 1365 (m), 1281 (m), 1248 (m), 1214 (m), 1135 (w), 1094 (m), 1060 (s), 1022 (w), 994 (w), 957 (m), 887 (m), 811 (m), 801 (m), 780 (s), 758 (s), 738 (m), 725 (m), 699 (w), 666 (w), 619 cm^{-1} (w); ESI-MS (pos. mode, MeCN): *m*/*z*: calcd for *M*H$^+$: 340.2137; found: 340.2127; elemental analysis calcd (%) for $C_{19}H_{25}N_5O$: C 67.23, H 7.42, N 20.63; found C 67.26, H 7.62, N 20.94.

[LFeCl$_2$] (1): **L** (800 mg, 2.36 mmol, 1 equiv) was added to a suspension of $FeCl_2$ (299 mg, 2.36 mmol) in THF (20 mL). The reaction mixture was stirred overnight and then the solution obtained was concentrated to a volume of 10 mL, which led to the deposition of a white precipitate of [LFeCl$_2$], **1**. The product was collected by filtration, washed with THF (2×5 mL), and dried to afford pure **1** in the form of a white solid (670 mg, 1.44 mmol, 61%). Crystals suitable for single-crystal X-ray diffraction studies could be obtained by evaporating the solvent from saturated solutions in THF or acetonitrile. According to the XRD results, these crystals contained one solvent molecule per two molecules of **1**. The crystals grown in THF were of better quality, and so Figure 1 relates to an investigation of these crystals. IR (KBr): $\tilde{\nu}$=3123 (m), 2974 (s), 2937 (m), 2913 (m), 2911 (m), 2908 (m), 2898 (m), 2866 (m), 2852 (w), 1586 (m), 1533 (m), 1496 (m), 1464 (m), 1431 (m), 1424 (m), 1377 (w), 1370 (m), 1246 (m), 1154 (m), 1101 (m), 1081 (s), 1071 (s), 1047 (w), 980 (m), 906 (m), 811 (m), 807 (m), 783 (s), 775 (m), 768 (m), 765 (m), 753 (m), 722 (w), 714 (m), 704 cm^{-1} (w); ESI-MS (pos. mode, MeCN): *m*/*z*: calcd for [*M*−Cl]$^+$: 430.1097; found: 430.1090; elemental analysis calcd (%) for crystals of **1** grown from CH_3CN, that is, **1**·0.5 CH_3CN ($C_{20}H_{26.5}Cl_2FeN_{5.5}O$): C 49.35, H 5.49, N 15.83, Cl 14.57; found C 49.37, H 5.46, N 15.61, Cl 14.62.

[LFeBr$_2$] (2): **L** (300 mg, 0.88 mmol, 1 equiv) was added to a solution of $FeBr_2$ (191 mg, 0.88 mmol) in THF (20 mL). The reaction mixture was stirred overnight and then the solution obtained was concentrated to a volume of 10 mL, which led to the deposition of a white precipitate of [LFeBr$_2$], **2**. The product was collected by filtration, washed with THF (2×5 mL), and dried to afford pure **2** in the form of a white solid (230 mg, 0.41 mmol, 47%); ESI-MS (pos. mode, MeCN): *m*/*z*: calcd for [*M*−Br]$^+$: 474.06383; found: 474.0581; elemental analysis calcd (%) for **2**·0.5 THF ($C_{21}H_{29}Br_2FeN_5O_{1.5}$): C 42.67, H 4.94, N 11.85, Br 27.03; found C 42.80, H 5.03, N 11.78, Br 24.87.

[LFeCl$_3$] (3): **L** (740 mg, 2.18 mmol, 1 equiv) was added to a solution of $FeCl_3$ (354 mg, 2.18 mmol) in THF (20 mL). The reaction mixture was stirred overnight and then the solution obtained was concentrated to a volume of 10 mL, which led to the deposition of a yellow-orange precipitate of [LFeCl$_3$], **3**. The product was collected by filtration, washed with THF (2×5 mL), and dried to afford pure **3** in the form of a yellow-orange solid (740 mg, 1.44 mmol, 68%). IR (KBr): $\tilde{\nu}$=3159 (m), 3138 (m), 3123 (m), 3100 (m), 3078 (m), 3016 (w), 2975 (m), 2971 (m), 2961 (m), 2937 (m), 2907 (m), 2870 (m), 2853 (m), 1599 (s), 1527 (m), 1490 (m), 1467 (m), 1440 (m), 1366 (m), 1274 (m), 1243 (m), 1213 (m), 1160 (w), 1131 (s), 1101 (m), 1093 (m), 1063 (m), 1051 (m), 1014 (w), 985 (m), 889 (m), 849 (m), 775 (m), 762 cm^{-1} (m); UV/Vis (acetonitrile) λ_{max1} (ε)= 313 nm (4310 M^{-1} cm^{-1}), λ_{max2} (ε)=356 nm (3820 M^{-1} cm^{-1}); ESI-MS (pos. mode, MeCN): *m*/*z*: calcd for [*M*−Cl]$^+$: 465.0786; found: 465.0777; elemental analysis calcd (%) for **3**·0.5 CH_2Cl_2 ($C_{19.5}H_{26}Cl_4FeN_5O$): C 43.04, H 4.82, N 12.87, Cl 26.06; found C 43.47, H 4.90, N 12.79, Cl 25.05.

Oxidative cleavage of 3,5-di-*tert*-butylcatechol (DBCH$_2$): In a typical reaction, **3** (45 mg, 0.09 mmol), $DBCH_2$ (20 mg, 0.09 mmol, 1 equiv), NEt_3 (25 μL, 0.18 mmol, 2 equiv), and sodium tetraphenylborate (31 mg, 0.09 mmol, 1 equiv) were dissolved in acetonitrile (30 mL) under an inert argon atmosphere in a glove box, and the reaction mixture was stirred for 5 min. Thereafter, excess O_2 was introduced and the mixture was stirred for a further 6 h. All volatiles were then removed under vacuum, and the residue was redissolved in $CHCl_3$. After filtration of this solution through silica gel, all volatiles were removed once more. One equivalent of naphthalene was added as a standard and the residue was analyzed by ^{1}H NMR spectroscopy, GC-MS, and GC-FID.[35] Data for 3,5-di-*tert*-butylquinone (**Q**): ^{1}H NMR ($CDCl_3$, 25°C): δ=1.23 (s, 9H), 1.28 (s, 9H), 6.22 (d, 1H), 6.93 ppm (d, 1H); data for 3,5-di-*tert*-butyl-1-oxacyclohepta-3,5-diene-2,7-dione (**A**): ^{1}H NMR ($CDCl_3$, 25°C): δ=1.17 (s, 9H), 1.29 (s, 9H), 6.15 (d, 1H), 6.45 ppm (d, 1H); CI-MS (methanol): *m*/*z*: 237.1 [*M*+H$^+$]; data for 4,6-di-*tert*-butyl-2-pyrone (**B**): ^{1}H NMR ($CDCl_3$, 25°C): δ=1.23 (s, 9H), 1.29 (s, 9H), 6.05 ppm (m, 2H); EI-MS: *m*/*z*= 208.1 [M^+]; CI-MS (methanol): *m*/*z*: 209.2 [*M*+H$^+$]; data for 3,5-di-*tert*-butyl-2-pyrone (**C**): ^{1}H NMR ($CDCl_3$, 25°C, ppm): δ=1.22 (s, 9H), 1.37 (s, 9H), 7.21 (d, 1H), 7.23 ppm (d, 1H); EI-MS: *m*/*z*: 208.1 [M^+]; CI-MS (methanol): *m*/*z*: 209.2 [*M*+H$^+$].

Acknowledgements

We are grateful to the Fonds der Chemischen Industrie, the Bundesministerium für Bildung, Wissenschaft, Forschung und Technologie, and the Dr. Otto Röhm Gedächtnisstiftung for financial support, as well as to Bayer GmbH, BASF AG, and Sasol GmbH for the supply of chemicals. We would also like to thank E. Hoppe, C. Knispel, P. Neubauer, and B. Ziemer for performing the crystal structure analyses, Prof. P. Wessig for carrying out analytical HPLC investigations, and C. Jankowski for preparing the starting materials. Finally, we acknowledge inspiring discussions with Professor Peter Comba and within the Cluster of Excellence "Unifying Concepts in Catalysis" funded by the DFG.

[1] H. Decker, T. Schweikardt, F. Tuczek, *Angew. Chem.* **2006**, *118*, 4658–4664; *Angew. Chem. Int. Ed.* **2006**, *45*, 4546–4550.
[2] W. N. Lipscomb, N. Sträter, *Chem. Rev.* **1996**, *96*, 2375–2433.
[3] A. L. Feig, S. J. Lippard, *Chem. Rev.* **1994**, *94*, 759–805.
[4] S. J. Lange, L. Que, Jr., *Curr. Op. Chem. Biol.* **1998**, *2*, 159–172; A. Beck, B. Weibert, N. Burzlaff, *Eur. J. Inorg. Chem.* **2001**, 521–527; M. M. Abu-Omar, A. Loaiza, N. Hontzeas, *Chem. Rev.* **2005**, *105*, 2227–2252; D. Oldenburg, C. Y. Ke, A. Tipton, A. A. Shteinman, L. Que, Jr., *Angew. Chem.* **2006**, *118*, 8143–8146; *Angew. Chem. Int. Ed.* **2006**, *45*, 7975–7978.
[5] S. Trofimenko, *Chem. Rev.* **1993**, *93*, 943–980.
[6] L. Zhou, D. Powell, K. M. Nicholas, *Inorg. Chem.* **2007**, *46*, 2316–2321.
[7] a) G. Anderegg, F. Wenk, *Helv. Chim. Acta* **1967**, *50*, 2330–2332; b) A. Diebold, K. S. Hagen, *Inorg. Chem.* **1998**, *37*, 215–223; S. Yan, D. D. Cox, L. L. Pearce, C. Juarez-Garcia, L. Que, Jr., J. H. Zhang, C. J. O'Connor, *Inorg. Chem.* **1989**, *28*, 2507–2509.

[8] I. G. Denisov, T. M. Makris, S. G. Sligar, I. Schlichting, *Chem. Rev.* **2005**, *105*, 2253–2277; P. R. Ortiz de Montellano, in *Cytochrome P450—Structure, Mechanism, and Biochemistry* (Ed.: P. R. Ortiz de Montellano), Plenum Press, New York, **1995**, pp. 245–303.
[9] M. Costas, M. P. Mehn, M. P. Jensen, L. Que, Jr., *Chem. Rev.* **2004**, *104*, 939–986.
[10] A. J. Canty, E. E. George, C. V. Lee, *Aust. J. Chem.* **1983**, *36*, 415–418.
[11] S. Trofimenko, J. C. Calabrese, J. S. Thompson, *Inorg. Chem.* **1987**, *26*, 1507–1514.
[12] R. Hüttel, P. Jochum, *Chem. Ber.* **1952**, *85*, 820–826.
[13] M. Wagner, C. Limberg, *Eur. J. Inorg. Chem.* **2008**, 3970–3976; C. D. Burbridge, D. M. L. Goodgame, *J. Chem. Soc. A* **1968**, 1074–1079; S. Hikichi, T. Ogihara, K. Fujisawa, N. Kitajima, M. Akita, Y. Moro-oka, *Inorg. Chem.* **1997**, *36*, 4539–4547; J. L. Kisko, T. Hascall, G. Parkin, *J. Am. Chem. Soc.* **1998**, *120*, 10561–10562.
[14] a) R. G. McDonald, M. A. Hitchman, *Inorg. Chem.* **1990**, *29*, 3074; b) T. Astley, A. J. Canty, M. A. Hitchman, G. L. Rowbottom, B. W. Skelton, A. H. White, *J. Chem. Soc. Dalton Trans.* **1991**, 1981.
[15] R. M. Acheson, *An Introduction to the Chemistry of Heterocyclic Compounds*, Wiley, New York, **1976**, p. 335.
[16] T. D. H. Bugg, G. Lin, *Chem. Commun.* **2001**, 941–952.
[17] Y. M. Chiou, L. Que, Jr., *Inorg. Chem.* **1995**, *34*, 3577–3578; D. H. Jo, Y. M. Chiou, L. Que, Jr., *Inorg. Chem.* **2001**, *40*, 3181–3190.
[18] a) P. C. A. Bruijnincx, M. Lutz, A. L. Spek, W. R. Hagen, G. von Koten, R. J. M. Klein Gebbink, *J. Am. Chem. Soc.* **2007**, *129*, 2275–2286; b) T. Ogihara, S. Hikichi, M. Akita, Y. Moro-oka, *Inorg. Chem.* **1998**, *37*, 2614–2615.
[19] a) M. Ito, L. Que, Jr., *Angew. Chem.* **1997**, *109*, 1401–1403; *Angew. Chem. Int. Ed. Engl.* **1997**, *36*, 1342–1344; b) D. H. Jo, L. Que, Jr., *Angew. Chem.* **2000**, *112*, 4454–4457; *Angew. Chem. Int. Ed.* **2000**, *39*, 4284–4287; c) P. C. A. Bruijnincx, M. Lutz, A. L. Spek, W. R. Hagen, G. von Koten, R. J. M. Klein Gebbink, *Inorg. Chem.* **2007**, *46*, 8391–8402; d) K. Visvaganesan, R. Mayilmurugan, E. Suresh, M. Palaniandavar, *Inorg. Chem.* **2007**, *46*, 10294–10306.
[20] a) L. Que, Jr., R. C. Kolanczyk, L. S. White, *J. Am. Chem. Soc.* **1987**, *109*, 5373–5380; b) D. D. Cox, L. Que, Jr., *J. Am. Chem. Soc.* **1988**, *110*, 8085–8092; c) H. G. Jang, D. D. Cox, L. Que, Jr., *J. Am. Chem. Soc.* **1991**, *113*, 9200–9204; d) M. Duda, M. Pascaly, B. Krebs, *Chem. Commun.* **1997**, 835–836; e) P. Mialane, L. Tchertanov, F. Banse, J. Sainton, J. J. Girerd, *Inorg. Chem.* **2000**, *39*, 2440–2444; f) W. O. Koch, H. J. Krüger, *Angew. Chem.* **1995**, *107*, 2928–2931; *Angew. Chem. Int. Ed. Engl.* **1996**, *34*, 2671–2674; g) M. Velusamy, R. Mayilmurugan, M. Palaniandavar, *Inorg. Chem.* **2004**, *43*, 6284–6293.
[21] D. D. Cox, S. J. Benkovic, L. M. Bloom, F. C. Bradley, M. J. Nelson, L. Que, Jr., D. E. Wallick, *J. Am. Chem. Soc.* **1988**, *110*, 2026–2032.
[22] T. Funabiki, Y. Nagai, H. Kojima, T. Tanaka, S. Yoshida, H. Masuda, *Inorg. Chim. Acta* **1998**, *275–276*, 222–229.
[23] G. Ackermann, D. Hesse, *Z. Anorg. Chem.* **1969**, *368*, 25–30.
[24] E. Mentasti, E. Pelizzetti, G. Saini, *J. Chem. Soc. Dalton Trans.* **1973**, 2609.
[25] R. Mayilmurugan, H. Stoeckli-Evans, M. Palaniandavar, *Inorg. Chem.* **2008**, *47*, 6645–6658.
[26] S. Mendel, A. Arndt, T. D. H. Bugg, *Biochemistry* **2004**, *43*, 13390–13396.
[27] S. L. Groce, J. D. Lipscomb, *Biochemistry* **2005**, *44*, 7175–7188.
[28] M. W. Vetting, L. P. Wackett, L. Que, Jr., J. D. Lipscomb, D. H. Ohlendorf, *J. Bacteriol.* **2004**, *186*, 1945–1958.
[29] J. S. Olson, A. J. Mathews, R. J. Rohls, B. A. Springer, K. D. Egeberg, S. G. Sligar, J. Tame, J. P. Renaud, K. Nagai, *Nature* **1988**, *336*, 265–266.
[30] The only synthetic complex that exclusively affords extradiol products is [Fe(Cl)(dtbc)(Me_3-tacn)], provided that 1 equiv of $AgBF_4$ is added to generate a vacant coordination site.[19b] This system seems to be quite exceptional, as in most cases both product types are found.
[31] M. Fujiwara, L. A. Golovleva, Y. Saeki, M. Nozaki, O. Hayashi, *J. Biol. Chem.* **1975**, *250*, 4848–4855.
[32] J. Schlosrich, K. L. Eley, P. J. Crowley, T. D. H. Bugg, *ChemBioChem* **2006**, *7*, 1899–1908.
[33] T. R. Demmin, M. M. Rogic, *J. Org. Chem.* **1980**, *45*, 1153–1156.
[34] Y. Tatsuno, M. Tatsuda, S. Otsuka, *J. Chem. Soc. Chem. Commun.* **1982**, 1100–1101.
[35] For the GC-MS/FID analysis, it is important that all $NaBPh_4$ is removed during the work-up procedure, as otherwise a reaction with any **Q** present in the sample occurs within the injector unit to give the boric ester (DBC)BPh. This would lead to a falsely suppressed yield of **Q**.

Received: December 10, 2008
Revised: February 19, 2009
Published online: April 9, 2009

